

# Optically induced multispin entanglement in a semiconductor quantum well

JIMING BAO<sup>1</sup>, ANDREA V. BRAGAS<sup>1</sup>, JACEK K. FURDYNA<sup>2</sup> AND ROBERTO MERLIN<sup>\*1</sup>

<sup>1</sup>FOCUS Center and Department of Physics, The University of Michigan, Ann Arbor, Michigan 48109-1120, USA

<sup>2</sup>Department of Physics, University of Notre Dame, Notre Dame, Indiana 46556, USA

\*e-mail: merlin@umich.edu

Published online: 23 February 2003; doi:10.1038/nmat839

According to quantum mechanics, a many-particle system is allowed to exhibit non-local behaviour, in that measurements performed on one of the particles can affect a second one that is far away. These so-called entangled states are crucial for the implementation of most quantum information protocols and, in particular, gates for quantum computation. Here we use ultrafast optical pulses and coherent techniques to create and control spin-entangled states in an ensemble of non-interacting electrons bound to donors (at least three) and at least two Mn<sup>2+</sup> ions in a CdTe quantum well. Our method, relying on the exchange interaction between localized excitons and paramagnetic impurities, can in principle be applied to entangle an arbitrarily large number of spins.

The problem of quantum entanglement has attracted much attention since the early days of quantum mechanics. One of the most intriguing features of this phenomenon is that non-interacting parts of a system can show non-local correlations reflecting interactions that occurred in the past (see, for example, ref. 1). Although techniques to entangle two particles and, in particular, two photons<sup>2</sup> have been known for some time, it is only recently that many (up to four)-particle entanglements have been demonstrated experimentally<sup>3,4</sup>. Following developments in quantum cryptography, together with the discovery of quantum algorithms that outperform those of classical computation, research on the foundations of quantum mechanics has now moved to the centre of the new field of quantum information<sup>5</sup>. As a result, the question of entanglement has gained practical significance.

In this work, we propose and demonstrate experimentally a novel method for many-particle entanglement involving Zeeman-split spin states of non-interacting paramagnetic impurities (Mn<sup>2+</sup> and donors) in a CdTe quantum well. Our approach relies on the exchange interaction between the impurity spin and excitons that are generated and controlled by optical means (for related mechanisms, see refs 6,7). As such, our scheme belongs to the category of entanglement mediated by an auxiliary quantum particle (for example, the centre-of-mass phonon in ion-trap quantum computers)<sup>4</sup>, as opposed to that resulting from the variation of parameters such as external fields or exchange constants<sup>8,9</sup>. Because the entangled spins do not interact with each other unless an exciton is present, our method distinguishes itself from other approaches where the sources of entanglement are interactions that cannot be controlled by the experimenter (for example, excitons in quantum dots<sup>10</sup> and NMR quantum computers<sup>5,11</sup>). Although our approach is, in principle, suitable for controlling the collective state of a single exciton-impurity system, the present study involves an inhomogeneous ensemble of excitons, each one mediating the interaction for the set of impurities that falls within its localization range.

Our entanglement proposal exploits the level diagram shown in Fig. 1, which was originally proposed<sup>12,13</sup> to explain multiple spin-flip Raman scattering in the same material system we use to demonstrate the method (mechanisms for multiple spin-flip Raman scattering are closely related to those for overtones of longitudinal optical phonons<sup>14</sup>).  $\vec{S} = (S_x, S_y, S_z)$  is the total spin of  $N$  bound electrons and  $B_e$  is an effective

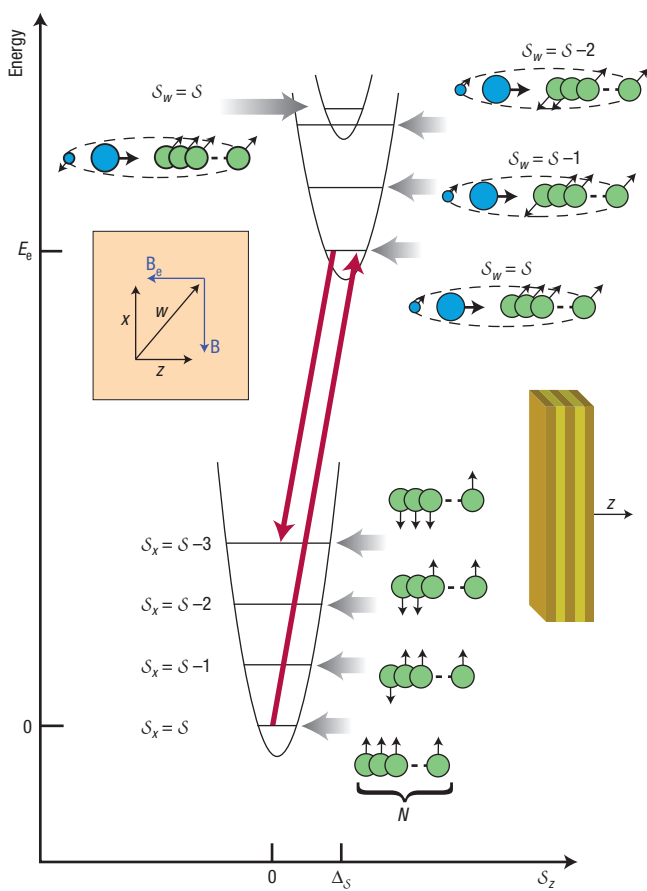


**Figure 1** Generic level structure of a system of paramagnetic impurities coupled to a single localized exciton in a quantum-well. Large (small) blue circles represent the hole (electron) in the exciton, of energy  $E_e$ . Bound electrons are represented by green circles. Optical transitions are depicted by red arrows and spins by arrows attached to the circles.  $S$  is the total spin quantum number. The diagram shows two exciton states differing in the orientation of the electron spin. Parabolas represent the vibrational analog for  $S \gg 1$ .

magnetic field describing the exchange coupling between the exciton and the impurities<sup>12,13,15</sup>. Central to our scheme is the requirement that  $B_e$  should not be parallel to the external field  $B$ , so that the quantization axes in the ground ( $x$  axis) and in the optically excited state ( $w$  axis) should not be the same, and that  $\langle S_z \rangle = \Delta_S \neq 0$  when the exciton is present. This is made possible by a combination of quantum confinement and spin-orbit coupling leading to heavy-hole states for which the hole-spin is parallel to the quantum-well  $z$  axis, irrespective of the orientation of  $B$ . (The heavy-hole states are the  $m_j = \pm 3/2$  eigenstates associated with the pseudo total angular momentum  $J$  with  $J = 3/2$ . For the heavy-hole spin to be oriented along the  $z$  axis, the splitting between the heavy and the  $m_j = \pm 1/2$  light-hole states must be large compared with the Zeeman splitting; this also applies to bulk wurtzite crystals and zinc-blende materials under strain)<sup>16</sup>. Because the eigenstates of  $S_x$  and  $S_w$  are not orthogonal to each other, this opens optical paths, such as the one shown by the red arrows in Fig. 1, that can be used to establish Raman coherences between an arbitrary pair of eigenstates of  $S_x$  and, independently, of  $S_w$ . Focusing for the moment on the  $S_x$  ladder, we then expect that a single, properly tailored optical pulse will be able to create entangled superposition states of the form

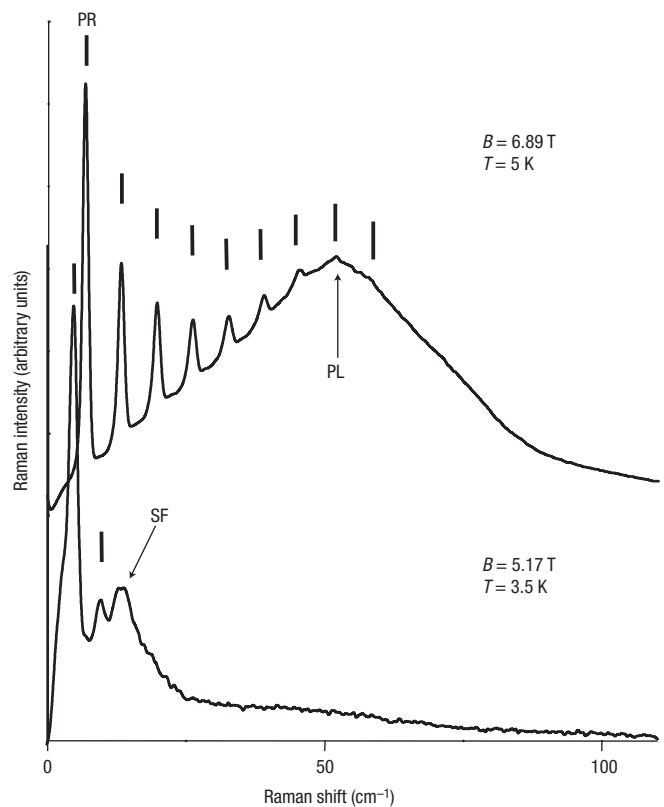


**Figure 2** Spontaneous resonant Raman scattering data. The spectra show multiples of the  $Mn^{2+}$ -paramagnetic resonance (PR). SF and PL denote, respectively, the spin-flip of a donor electron and photoluminescence due to localized excitons. The laser energy is 1.685 eV and 1.659 eV for the top and bottom spectra, respectively.

$$\Psi = \sum_{k=0}^{2S} C_k e^{-ik\Omega_0 t} |S-k\rangle \quad (1)$$

with predetermined values for the coefficients  $C_k$ , where  $k$  is an integer and  $t$  is time. Here,  $|S-k\rangle$  is the eigenstate of  $S_x$  of eigenvalue  $(S-k)$  and  $\Omega_0 = g\mu_B B/\hbar$ , where  $g$  is the gyromagnetic factor and  $\mu_B$  is the Bohr magneton. Note that  $|\hat{S}|^2\Psi = S(S+1)\Psi$  and that states with different values of  $S$  are orthogonal to each other. We also emphasize the fact that, although  $\Psi$  contains  $2S$  independent coefficients  $C_k$ , the associated product states have only one independent variable, because the coherent superposition is symmetric under spin exchange. Therefore,  $\Psi$  is entangled except for a set of  $C_k$  values of measure zero.

We stress the fact that a single pulse can create simultaneously  $S_x$  and  $S_w$  Raman coherences. In time-domain measurements, the signature for a Raman coherence involving states  $|S-j\rangle$  and  $|S-l\rangle$  is the observation of oscillations of frequency  $|j-l|\Omega_0$ . Note that, for donors (spin  $\sigma = 1/2$ ), the  $m$ th harmonic of  $\Omega_0$  is associated with an entanglement involving at least  $m$  impurities. For  $S \gg 1$ , we can map the problem into that of harmonic oscillators displaced by  $\Delta_S$  with respect to each other, as represented by the parabolas in Fig. 1. Thus, the Hamiltonian becomes identical to that of a molecule with electrons that couple to a single vibrational mode. The associated Huang–Rhys factor is given by  $\Delta_S^2/2 = S(1 + B^2/B_e^2)^{-1/2}$ . This mapping is important, for it allows us to use the vast literature on coherent molecular spectroscopy (particularly time-domain studies<sup>17,18</sup>) to analyse our experimental results.

The measurements were performed on a multiple quantum well structure consisting of 100 periods of  $Cd_{0.997}Mn_{0.003}Te$  wells of thickness

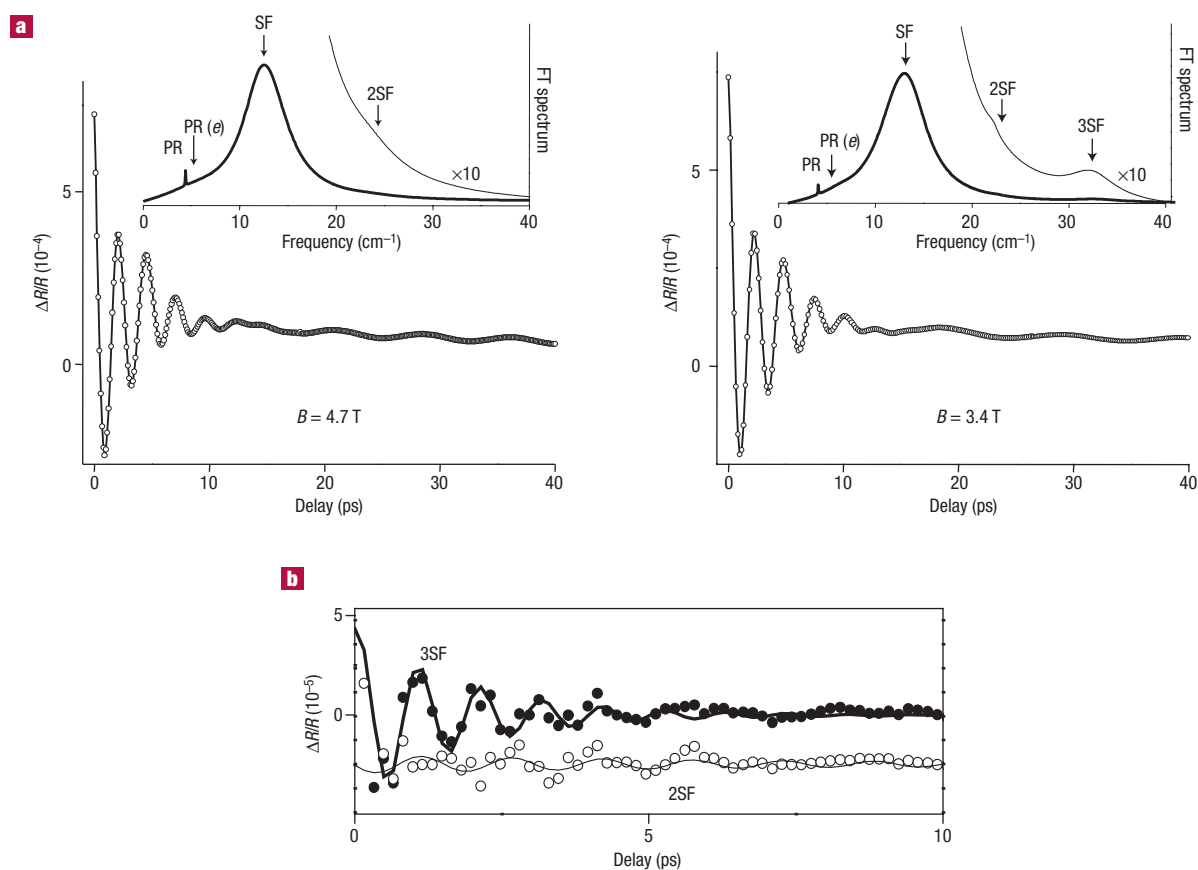


**Figure 3** Time-domain experiments. **a**, Differential reflectivity data at  $\hbar\omega_c = 1.687$  eV (open circles) for two different external magnetic field strengths ( $B$ ). Curves are fits using the linear prediction method<sup>25,26</sup>. The mode parameters gained from the fits were used to generate the Fourier transform (FT) spectra. The dominant SF peak is a doublet associated with electron spin-flips. Its lower-frequency component, due to electrons bound to donors, exhibits harmonics at twice (2SF) and three times (3SF) the fundamental frequency (data has been multiplied by ten for clarity). **b**, Data at 3.4 T showing SF-overtones. These results were obtained by subtracting the fitted contributions of all other oscillations.

58 Å, and MnTe barriers of thickness 19 Å grown in the [001]  $z$  direction (for a review of diluted magnetic semiconductors, see ref. 19). The  $\text{Mn}^{2+}$  ions were not intentionally introduced in the wells during growth. The presence of  $\text{Mn}^{2+}$  ions there is due to diffusion from the MnTe barriers with an interface broadening length of, typically, 1–2 monolayers<sup>20</sup>. The sample is nominally undoped. Consistent with other reports<sup>12,13,21,22</sup>, however, our Raman scattering experiments reveal the presence of isolated donors in the wells. We used a continuous wave Ti-sapphire laser to acquire Raman scattering, photoluminescence, and photoluminescence excitation spectra, as well as a mode-locked Ti-sapphire laser (emitting subpicosecond pulses) in a standard pump-probe set-up to obtain time-domain differential reflectivity data. Changes in the intensity of the reflected probe pulse,  $\Delta R$ , give a measure of the dependence of the optical constants on the coefficients  $C_k$  characterizing the particular entangled states created by the pump. Following the molecular nomenclature, the entangled states with and without excitons will be referred to in the following as ‘excited-state’ and ‘ground-state’ coherences. Processes by which ground-state coherences modulate the probe signal are impulsive stimulated Raman scattering and its associated imaginary component, nonlinear absorption. Excited-state coherences modulate the spectrum of stimulated emission<sup>17,18</sup>.

Figure 2 shows resonant Raman results obtained in the Voigt geometry. Depending on the laser energy, the spectrum shows up to

~10 lines at multiples of the  $\text{Mn}^{2+}$  paramagnetic resonant (PR) frequency and, in addition, a peak at  $\sim 13$   $\text{cm}^{-1}$  due to the spin-flip of an electron bound to a donor. The PR scattering is strongly enhanced when the energy of the scattered photon resonates with the main photoluminescence feature at the exciton energy  $E_c \sim 1.677$  eV, associated with dipole-allowed transitions involving heavy-hole states. Our Raman scattering results are in excellent agreement with work reported<sup>12,13</sup> on similar samples. In particular, we find that the position of the photoluminescence is red-shifted (by  $\sim 6$  meV at  $B=0$ ) with respect to the maximum of the photoluminescence excitation spectrum, indicating that the relevant intermediate states of the Raman process are localized excitons. Consistent with the model depicted in Fig. 1, the multiple PR-scattering is not observed in the Faraday geometry where the hole quantization axis,  $B$  and  $B_c$  are all along  $z$ . We recall that the peaks involving an odd (even) number of  $\text{Mn}^{2+}$  spin-flips are observed mainly when the polarizations of the incident and scattered light are perpendicular (parallel) to each other<sup>12,13</sup>. This agrees with the fact that the corresponding excitations are odd (even) under time-reversal and, hence, that they belong to the antisymmetric  $A_2$  (symmetric  $A_1$ ) representation of the  $D_{2d}$  point group of the quantum well (however, a departure from this symmetry is observed at very low temperatures)<sup>12,13</sup>.

Figure 3 shows time-domain data obtained in the Voigt geometry using a circularly polarized pump, which couples to only one of the two

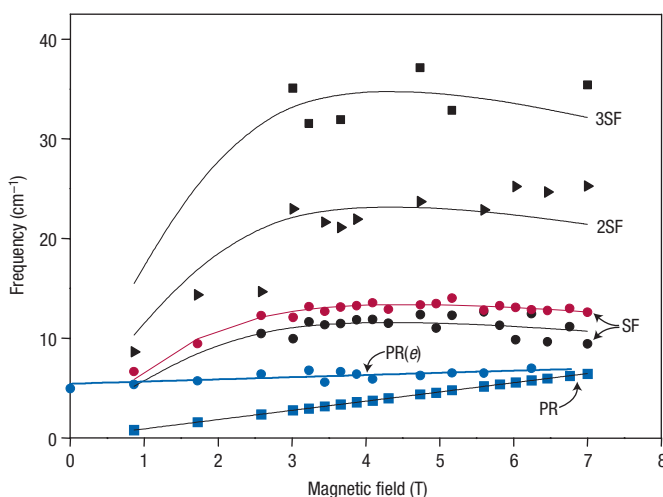


**Figure 4** Frequency versus magnetic field. Black (red) symbols represent spin-flips of donor (exciton) electrons. Associated curves are fits using the Brillouin function; see Methods.  $\text{Mn}^{2+}$ -transitions are shown in blue. Lines are linear fits to the data.  $\hbar\omega_c = 1.687$  eV.

$m_j = \pm 3/2$  states, and a probe detection scheme for which only antisymmetric  $A_2$  excitations are allowed (we used the differential Faraday rotation method<sup>23</sup>; it can be shown that the corresponding geometry allows for  $A_2$ - but not  $A_1$ -symmetry excitations). We worked at sufficiently low laser fluences so that the normalized differential reflectivity,  $\Delta R/R$ , depends linearly on the pump, and is independent of the probe intensity. The long-lived oscillations are due to the  $\text{Mn}^{2+}$  PR-transition. At short times, the signal is dominated by electron Zeeman quantum beats, that is, oscillations showing field and temperature behaviour consistent with that of spin-flips of electrons. The corresponding feature in the Fourier transform (FT) spectrum is labelled SF. These results bear a close resemblance to those reported for (Zn,Cd,Mn)Se heterostructures for which the rapidly decaying oscillations were ascribed to free photoexcited electrons<sup>24</sup>. However, close inspection of the data brings out important differences concerning the nature of the oscillations as well as the source of the coherence. As shown in Fig. 3, linear prediction fits<sup>25,26</sup> reveal that the dominant SF feature is actually a doublet at  $\sim 12$  and  $13$   $\text{cm}^{-1}$  ( $B = 7$  T), and that there are additional contributions due to a mode labelled PR( $e$ ) whose frequency depends weakly on the field and, most strikingly, peaks 2SF and 3SF that appear at nearly twice and three times the frequency of SF. These modes do not appear in the Raman scattering spectra but, like the Raman features, their amplitudes exhibit a large enhancement when the central energy of the pulses,  $\hbar\omega_c$ , is tuned to resonate with the photoluminescence associated with localized states.

For reasons discussed in the following, we assign all but the PR( $e$ )-feature and one of the components of the SF doublet to spin-flip ground-state coherences. Explicitly, we ascribe the low- (high-) frequency component of the SF doublet to the spin-flip of the electron that belongs to the donor (exciton); the PR( $e$ ) mode to the  $\text{Mn}^{2+}$  transition in the excited state; and the 2SF and 3SF modes to multiple spin-flips of donors. Because the electron spin is  $\sigma = 1/2$ , the observation of the SF-overtones indicates the establishment of Raman coherences and, hence, entanglement involving at least three donor impurities. Because the spectrum of localized excitations is very susceptible to  $\text{Mn}^{2+}$  density fluctuations, and also depends on the positions of the localization centres in the quantum well, we believe that the fast decay of all but the PR-mode is caused by inhomogeneous broadening.

We further note that, in terms of the vibrational analog<sup>15</sup>, the excited quantum oscillator in the impulsive limit is in a coherent state<sup>17,18</sup>. This, and the fact that the two-ion spin system ( $S = 5$ ) is well described by a harmonic oscillator whereas the three-donor case ( $S = 1.5$ ) is strongly anharmonic, offers an explanation as to why overtones occur for the donors but not the  $\text{Mn}^{2+}$  ions.

To further substantiate our assignments, consider the heavy-hole component of the exchange interaction  $V_{\text{HH}} = (\beta/3)\sum_i \delta(\mathbf{r} - \mathbf{r}_i)\mathbf{S}(\mathbf{r}_i)\cdot\mathbf{J}$  between a quantum well exciton and  $\text{Mn}^{2+}$  ions of spin  $S$  at sites  $\mathbf{r}_i$ . Here,  $\delta$  is the Dirac function,  $\beta$  is a constant, and  $\mathbf{r}$  is the coordinate<sup>19</sup>. As mentioned earlier, the effect of  $V_{\text{HH}}$  on the ions can be expressed in terms of an effective field  $\mathbf{B}_e(\mathbf{r}) = (\beta/3\mu_B g_{\text{Mn}})|\Psi_{\text{HH}}(\mathbf{r})|^2\mathbf{J}$  where  $g_{\text{Mn}} \approx 2$  and  $\Psi_{\text{HH}}$  is the hole wavefunction<sup>12,13</sup>. Hence, in the presence of the exciton the paramagnetic transition energy evolves from  $\mu_B g_{\text{Mn}} B_e$  at  $B = 0$  to  $\mu_B g_{\text{Mn}} B$  for  $B \gg B_e$ . The latter is consistent with the asymptotic behaviour and the basis for assigning the PR( $e$ ) peak to the  $\text{Mn}^{2+}$  spin-flip transition in the excited state. From the PR( $e$ ) frequency at zero field and using for CdTe  $n_0\beta = 0.88$  eV, where  $n_0$  is the number density of unit cells (ref. 19), we obtain the very reasonable estimate of  $\sim 40$  Å for the hole localization length (the bulk exciton radius in CdTe is 50 Å) leading on average to 2.5  $\text{Mn}^{2+}$  ions per hole. From this number, the Huang–Rhys factor we infer is  $\sim 1.06$  ( $B = 7$  T) which is consistent with the observation of  $\sim 10$  overtones in the Raman spectrum. Albeit indirect, the combination of the Raman scattering and coherent results gives strong evidence for exciton-mediated entanglement involving at least two  $\text{Mn}^{2+}$  ions.

Our assignment of the SF doublet, 2SF and 3SF, as being due to the spin-flips of donor-bound electrons is supported, first, by the observation that these features resonate at  $\hbar\omega_c \approx E_c$  and, second, by their dependence on temperature and field, which show excellent agreement with theoretical predictions. The curves in Fig. 4 are fits using the standard Brillouin function to account for  $\langle \mathbf{S}\cdot\mathbf{B} \rangle$  in the expression for the effective electron parameter  $g_e$  (see Methods). The resonant behaviour is a clear indication that the relevant states are localized. This, and the linear dependence of the signal with the pump intensity are consistent with the donor interpretation for 2SF and 3SF, because linearity excludes the possibility that the overtones could be due to multiple spin-flips of bound excitons. Additional proof is given by the fact that 2SF is usually much weaker than 3SF; see Fig. 3. This supports our assignment because double-flip excitations transform like  $A_1$  and, therefore, are nominally forbidden in the geometry we used (all other modes, being single or triple flips, belong to the  $A_2$  representation). On the basis of the value of the frequencies at large fields, the fundamental mode from which 2SF and 3SF derive is ascribed to the lower-frequency component of the SF doublet. This mode and the overtones exhibit a similar  $\hbar\omega_c$  behaviour, different to that of the higher-frequency component associated with the spin-flip of the electron in the bound exciton (see Fig. 1). The fact that the energy of the latter is slightly larger is attributed to exchange effects in the excited-state. From the measured splitting, we obtain an upper limit of  $\sim 600$   $\mu\text{eV}$  for the electron–hole exchange that is consistent with the value 270  $\mu\text{eV}$  from the literature<sup>27</sup>. This estimate ignores electron–electron exchange, which is large for exciton–donor complexes<sup>28</sup> and may provide an additional longer-range mechanism for donor entanglement.

To provide a quantitative estimate of the entanglement, we neglect absorption and write the effective interaction of light with bound electrons as  $\sum_{S,k,l} H_S(k, l)$  where

$$H_S(k, l) = E^2(t) \times \left\{ \sum_{uv, \eta} e_u e_v R_{uv}^{\eta}(k, l) |\eta, S-k\rangle \langle \eta, S-l| + c.c. \right\}. \quad (2)$$

The sum is over all sets of  $N$  ( $\equiv 2S$ ) electrons, each set denoted by  $\eta$ .  $\mathbf{E}$  is the electric field,  $\mathbf{e} = \mathbf{E}/E$  is a unit vector of components  $e_u$ ,  $R_{uv}^{\eta}(k, l)$  is the Raman tensor for the corresponding transition of the particular set (this tensor vanishes unless all the impurities in the set interact with a single exciton), and  $c.c.$  is the complex conjugate. Consider a weak impulsive excitation and zero temperature. Then, if  $|0\rangle$  is the wave function

immediately before the pulse strikes (the ground state with all spins aligned along B), integration of Schrödinger equation gives for  $t > 0$  the coherent superposition state

$$\Phi \approx |0\rangle + iI_0 \sum_{\mathcal{S} \geq k > 0, \eta} \Xi_{\eta k} |\eta, \mathcal{S} - k\rangle \exp(-ik\Omega_0 t) \quad (3)$$

which is entangled for most values of the integrated intensity of the pump pulse,  $I_0$ . Here,  $\Xi_{\eta k} = (4\pi / n_R c\hbar) \sum_{uv} e_u e_v R_{uv}^{\eta}(k, 0)$  and  $n_R$  is the refractive index, and  $c$  is the speed of light. A secondary effect of the interaction is that  $\Phi$  leads to time-varying optical constants (see, for example, ref. 29) with concomitant oscillations in the intensity of the reflected probe pulse. Explicitly,

$$\Delta R/R \propto I_0 \sum_k |\Xi_{\eta k}|^2 \exp(-ik\Omega_0 t) \quad (4)$$

For a given set of impurities, and to lowest order in  $I_0$ , the only non-zero components of the density matrix operator,  $\hat{\rho}_{\eta}(k, l) = |\eta, \mathcal{S} - k\rangle\langle\eta, \mathcal{S} - l|$ , are  $\langle\Phi|\hat{\rho}_{\eta}(0, 0)|\Phi\rangle \approx 1$  and  $\langle\Phi|\hat{\rho}_{\eta}(k, 0)|\Phi\rangle = \langle\Phi|\hat{\rho}_{\eta}(0, k)|\Phi\rangle^* = -iI_0 \Xi_{\eta k} \exp(-ik\Omega_0 t)$ . Let  $\mathcal{N}_m$  be the number of sets of  $m$  impurities. Defining the ensemble average

$$\rho(m) = \sqrt{\sum_{\eta} |\langle\Phi|\hat{\rho}_{\eta}(m, 0)|\Phi\rangle|^2 / \mathcal{N}_m} \quad (5)$$

it follows that the amplitude of the  $m$ th-harmonic oscillations gives a direct measure of the entanglement because it is proportional to  $|\rho(m)|^2$ . From the results for donors at 3.4 T (Fig. 3), we get  $\langle\rho(2)\rangle/\langle\rho(1)\rangle \approx 0.014$  and  $\langle\rho(3)\rangle/\langle\rho(1)\rangle \approx 0.46$  (because the evidence for entanglement is indirect, values for  $\text{Mn}^{2+}$  cannot be directly inferred from the experiments). It is important to realize that the strength of the  $m$ th harmonic also measures the probability of finding  $m$  donors in the region where the coupling between the localized exciton and the impurities is significant. Assuming an interaction length of  $\sim 100$  Å (in CdTe, the donor radius is  $\sim 50$  Å), the ratio between the frequency-integrated intensities of the first (SF) and third harmonic (3SF) gives the crude estimate of  $5 \times 10^{16} \text{ cm}^{-3}$  for the density of donors in our sample. Using this density, we obtain  $\langle\rho(1)\rangle / I_0 \approx 30 \text{ m}^2 \text{ J}^{-1}$ , which is  $\sim 10^3$ – $10^4$  larger than the value calculated for off-resonance excitation.

In conclusion, our results confirm that there is a system of localized excitons coupled to paramagnetic impurities in a CdTe quantum well that is well described by the level structure of Fig. 1. We have shown that such a system can be optically excited to generate many-spin Raman coherences for an ensemble. Because the exciton localization centres (due to, for example, surface roughness) and the impurities do not necessarily overlap, our scheme can in principle be applied to entangle a particular group and, ultimately, a large number of spins by using one exciton at a time to address different sets of impurities. Hence, the procedure is potentially set-specific and scalable, thereby holding promise for quantum computing applications.

## METHODS

The mode-locked Ti-sapphire laser (Spectra Physics, Tsunami), pumped by a continuous wave 532 nm, 5 W, diode-pumped solid-state laser (Spectra Physics Millennia), provided  $\sim 130$  fs pulses at a repetition rate of 82 MHz, which were focused to a spot of 400  $\mu\text{m}$  diameter using an average power of 3–4 mW. The home-built, continuous wave Ti-sapphire source operated at power densities of  $\sim 10^2 \text{ W cm}^{-2}$ . The laser range covers the fundamental gap of the wells, at  $\sim 1.68$  eV. Data were obtained either in the Voigt (BLz) or the Faraday (B//z) geometry with the photon wavevector along z.

## MAGNETIC FIELD BEHAVIOUR

The dominant features of both spontaneous Raman and coherent time-domain spectra are intra-well excitations involving the  ${}^6S_{5/2}$ -multiplet of  $\text{Mn}^{2+}$  and spin-flips associated with states derived from the conduction band. The field dependence of these transitions is given by the Zeeman coupling  $\mu_B \mathbf{B} \cdot (\mathbf{g}_\sigma \sigma + \mathbf{g}_S \mathbf{S})$  where  $\sigma$  and  $\mathbf{S}$  are, respectively, the electron spin of the donor ( $\sigma = 1/2$ ) and the  $\text{Mn}^{2+}$  ions ( $S = 5/2$ ) with  $g_{\text{Mn}} = 2$  (ref. 19). The parameter  $g_e = \tilde{g} - n_0 \alpha x (\mathbf{S} \cdot \mathbf{B}) / \mu_B B^2$  is an effective factor that accounts

for the exchange interaction of the donor electron with the  $\text{Mn}^{2+}$ -spins. Here  $\tilde{g}_e \approx -1.64$  is the bare g-factor,  $x$  is the  $\text{Mn}^{2+}$  concentration and  $n_0$  is the density of unit cells; for CdTe,  $n_0 \alpha \approx 0.22$  eV (ref. 19). Coupling to the  $\text{Mn}^{2+}$  ions leads to a strongly nonlinear dependence of the Zeeman levels with B, characterized by saturation, that can be used to determine the  $\text{Mn}^{2+}$  concentration as well as to distinguish electron spin-flip from other features (note that the g-factor has approximately the same value for free electrons, electrons bound to donors and electrons in free and bound excitons)<sup>19</sup>.

Received 29 November 2002; accepted 22 January 2003; published 23 February 2003.

## References

- Wheeler, J. A. & Zurek, W. H. (eds) *Quantum Theory and Measurements* (Princeton Univ. Press, Princeton, 1983).
- Kwiat, P. G., Berglund, A. J., Altepeter J. B. & White, A. G. Experimental verification of decoherence-free subspaces. *Science* **290**, 498–501 (2000).
- Rauschenbeutel, A. *et al.* Step-by-step engineered multiparticle entanglement. *Science* **288**, 2024–2028 (2000).
- Sackett, C. A. *et al.* Experimental entanglement of four particles. *Nature* **404**, 256–259 (2000).
- Nielsen, M. A. & Chuang, I. L. *Quantum Computation and Quantum Information* (Cambridge Univ. Press, Cambridge, 2000).
- Piermarocchi, C., Chen, P., Sham, L. J. & Steel, D. G. Optical RKKY Interaction between Charged Semiconductor Quantum Dots. *Phys. Rev. Lett.* **89**, 167402 (2002).
- DiVincenzo, D. P., Bacon, D., Kempe, J., Burkard, G. & Whaley, K. B. Universal quantum computation with the exchange interaction. *Nature* **408**, 339–342 (2000).
- Burkard, G., Loss D. & DiVincenzo, D. P. Coupled quantum dots as quantum gates. *Phys. Rev. B* **59**, 2070–2078 (1999).
- O'Brien, J. L. *et al.* Towards the fabrication of phosphorus qubits for a silicon quantum computer. *Phys. Rev. B* **64**, R161401 (2001).
- Chen, G. *et al.* Optically induced entanglement of excitons in a single quantum dot. *Science* **289**, 1906–1909 (2000).
- Vandersypen, L. M. K. *et al.* Experimental realization of Shor's quantum factoring algorithm using nuclear magnetic resonance. *Nature* **414**, 883–887 (2001).
- Stühler, J. *et al.* Multiple  $\text{Mn}^{2+}$ -spin-flip Raman scattering at high fields via magnetic polaron states in semimagnetic quantum wells. *Phys. Rev. Lett.* **74**, 2567–2570 (1995); Erratum. *Phys. Rev. Lett.* **74**, 4966 (1995).
- Stühler, J. *et al.* Polarization properties of multiple  $\text{Mn}^{2+}$ -spin-flip Raman scattering in semimagnetic quantum wells. *J. Cryst. Growth* **159**, 1001–1004 (1996).
- Merlin, R. *et al.* Multiphonon processes in YbS. *Phys. Rev. B* **17**, 4951–4958 (1978).
- Kavokin, K. V. & Merkulov, I. A. Multispin Raman paramagnetic resonance: Quantum dynamics of classically large angular momenta. *Phys. Rev. B* **55**, R7371–R7374 (1997).
- Martin, R. W. *et al.* Two-dimensional spin confinement in strained-layer quantum wells. *Phys. Rev. B* **42**, 9237–9240 (1990).
- Kumar, A. T. N., Rosca, F., Widom A. & Champion, P. M. Investigations of amplitude and phase excitation profiles in femtosecond coherence spectroscopy. *J. Chem. Phys.* **114**, 701–724 (2001).
- Pollard, W. T., Lee S. Y. & Mathies, R. A. Wave packet theory of dynamic absorption spectra in femtosecond pump-probe experiments. *J. Chem. Phys.* **92**, 4012–4029 (1990).
- Furdyna, J. K. Diluted magnetic semiconductors. *J. Appl. Phys.* **64**, R29–R64 (1988).
- Adleff, A., Hendorfer, G., Jantsch, W. & Faschinger, W. Diffusion of Mn-atoms during the growth of CdTe-MnTe superlattices. *Mater. Sci. Forum* **143–147**, 1409–1413 (1994).
- Kusrayev, Y. G., Koudinov, A. V., Wolverson, D. & Kossut, J. Anisotropy of spin-flip Raman scattering in CdTe/CdMnTe quantum wells. *Phys. Status Solidi* **229**, 741–744 (2002).
- Ramdas, A. K. & Rodriguez, S. in *Light Scattering in Solids VI* (eds Cardona M. & Güntherodt G.) Ch. 4. 137–206 (Springer, Berlin, 1991).
- Crooker, S. A., Awschalom, D. D. & Samarth, N. Time-resolved Faraday rotation spectroscopy of spin dynamics in digital magnetic heterostructures. *IEEE J. Sel. Top. Quant.* **1**, 1082–1092 (1995).
- Crooker, S. A., Awschalom, D. D., Baumberg, J. J., Flack, F. & Samarth, N. Optical spin resonance and transverse spin relaxation in magnetic semiconductor quantum wells. *Phys. Rev. B* **56**, 7574–7588 (1997).
- Barkhuijsen, H., De Beer, R., Bovée, W. M. M. J. & van Ormondt, D. Retrieval of frequencies, amplitudes, damping factors, and phases from time-domain signals using a linear least-squares procedure. *J. Mag. Res.* **61**, 465–481 (1985).
- Wise, F. W., Rosker, M. J., Millhauser, G. L. & Tang, C. L. Application of linear prediction least-squares fitting to time-resolved optical spectroscopy. *IEEE J. Quant. Elect.* **23**, 1116–1121 (1987).
- Besombes, L., Kheng, K. & Martrou, D. Exciton and biexciton fine structure in single elongated islands grown on a vicinal surface. *Phys. Rev. Lett.* **85**, 425–428 (2000).
- Benoit à la Guillaume, C. & Lavallard, P. Excited states of an exciton bound to a neutral donor. *Phys. Status Solidi B* **70**, K143–K145 (1975).
- Boyd, R. W. *Nonlinear Optics*. Ch. 9, 365–397 (Academic, San Diego, 1992).

## Acknowledgements

We acknowledge support from The Petroleum Research Fund, administered by the ACS (American Chemical Society), for partial support of this research. Work also supported by the NSF (National Science Foundation) under Grants No. PHY 0114336 and No. DMR 0072897, by the AFOSR (Air Force Office of Scientific Research) under contract F49620-00-1-0328 through the MURI program and by the DARPA-SpinS program. A.V.B. acknowledges partial support from CONICET (Consejo Nacional de Investigaciones Científicas y Técnicas, Argentina). Correspondence and requests for materials should be addressed to R.M.

## Competing financial interests

The authors declare that they have no competing financial interests.